Emission Source Areas of Fine Particulate Matter (PM$_{2.5}$) in Ho Chi Minh City, Vietnam

Tuyet Nam Thi Nguyen [1,*] **, Nguyen Xuan Du** [2] **and Nguyen Thi Hoa** [1]

1   Faculty of Environment, Saigon University (SGU), Ho Chi Minh City 74900, Vietnam
2   Division of Project and Infrastructure Management, Saigon University (SGU),
     Ho Chi Minh City 74900, Vietnam
*   Correspondence: ntnam@sgu.edu.vn; Tel.: +84-779534930

Abstract: This study aims to determine emission source areas of fine particulate matter (PM$_{2.5}$) in Ho Chi Minh (HCM) City, Vietnam, using a conditional bivariate probability function (CBPF) and hybrid receptor models, including three-dimensional potential source contribution function (3D-PSCF) and concentration-weighted trajectory (3D-CWT), considering latitudes, longitudes, and height of trajectory segments. Uncertainties of the CBPF and 3D-PSCF/3D-CWT were evaluated based on the 95th confidence intervals and 95% confidence levels, respectively. For the local scale, PM$_{2.5}$ in HCM City was primarily emitted from shallow or common ground sources (e.g., vehicle emissions) throughout the year. Regarding non-local source areas, PM$_{2.5}$ in HCM City is contributed by those originated from the East Sea (e.g., shipping emissions) and southeastern Vietnam (e.g., Binh Duong and Dong Nai provinces) having several industrial zones with PM$_{2.5}$ emission sources, especially in the dry season (December to April of the following year). In the rainy season (May–November), PM$_{2.5}$ derived from emission sources in the Mekong Delta (e.g., biomass burning) might be transported to HCM City. However, contribution of the non-local sources to PM$_{2.5}$ pollution in HCM City during the rainy season is less important because of PM$_{2.5}$ deposition stemmed from the high rainfall amount in this season.

Keywords: PM$_{2.5}$; emission source area; CBPF; 3D-PSCF; 3D-CWT; Ho Chi Minh City

1. Introduction

Vietnam is situated in Southeast Asia, bordered to the west by Laos and Cambodia and to the north by China. The Vietnamese economy is one of the most rapidly rising in Asia. Additionally, Vietnam has become a long-term desirable market because of its average annual growth rate of gross domestic product, steady population growth, and prosperity increase [1]. Most of Vietnam's area is covered by mountains and hills, with the remainder being flat plains. In addition, the topography of Vietnam diminishes from the northwest to the southeast, causing Vietnamese's climate to change significantly according to latitude and relief [2]. Particularly, northern Vietnam experiences significant temperature variations among seasons (i.e., spring, summer, fall, and winter), whereas southern Vietnam is mostly warm throughout the year and has two seasons per year (i.e., dry and rainy seasons) [3].

Ho Chi Minh (HCM) City, located in southern Vietnam, is the political, economic, and cultural hub of the country. Due to its high population and traffic density [4], HCM City has faced several environmental problems, including air pollution. The levels of air pollutants in HCM City, such as particulate matter (PM), nitrogen oxide (NO$_x$), sulphate dioxide (SO$_2$), carbon monoxide (CO), and ozone (O$_3$), were reported to noticeably exceed the thresholds for air pollutants introduced by the World Health Organization (WHO) and Vietnamese government [5–7]. In particular, considering the global air quality guidelines suggested by WHO, the 24 h (annual) average concentrations of PM$_{2.5}$ (PM lower than 2.5 µm), PM$_{10}$ (PM lower than 10 µm), NO$_2$, and SO$_2$ are 15 (5), 45 (15), 25 (10), and

40 μg m^{-3}, respectively [8]. For the Vietnamese air quality guidelines, the thresholds for 24 h (annual) average concentrations of PM$_{2.5}$, PM$_{10}$, NO$_2$, and SO$_2$ are 50 (25), 150 (50), 100 (40), and 125 (50) μg m^{-3}, respectively [9]. Regarding air pollution in HCM City, the 24 h (annual) average concentrations of PM$_{2.5}$, PM$_{10}$, NO$_2$, and SO$_2$ were reported as (36.3), 73, 22, and 22 μg m^{-3}, respectively [5,6]. These concentrations relatively reached the thresholds issued by the Vietnamese government but were 2–6 times higher than the those introduced by WHO. Thus, exposure to these pollutants (i.e., PM, NO$_x$, SO$_2$, CO, and O$_3$) through inhalation and/or dermal contact can adversely affect human health. Of these pollutants, fine particulate matter, also called PM$_{2.5}$, is one of the most frequently monitored pollutants [10] because compositions of PM$_{2.5}$ can contain several toxic chemicals, such as trace metals (e.g., arsenic, lead, and mercury), organic compounds (e.g., polycyclic aromatic hydrocarbons and polychlorinated biphenyls), and inorganic compounds (e.g., anions and cations). In addition, PM$_{2.5}$ has a small size (i.e., lower than 2.5 μm), thus, it can deeply penetrate the human respiratory system and cause many diseases, such as lung irritation, coughing, asthma, and lung cancer [11].

Based on the emission inventory analysis, PM$_{2.5}$ in HCM City has been noted to be mainly emitted from transportation activities, industrial productions, and household emissions [12–14]. Additionally, according to directions of backward air trajectories, several regions were reported to be the possible emission source areas of PM$_{2.5}$ in HCM City, such as the Mekong Delta at southwestern HCM City [5,15], and some provinces in southeastern Vietnam, including Binh Duong, Dong Nai, and Binh Phuoc provinces [14]. However, to improve the accuracy of source area identification, the backward air trajectories should be associated with PM$_{2.5}$ concentrations at the receptor site [16]. Moreover, information on determining the emission source areas of PM$_{2.5}$ in HCM City using receptor models, linking air parcels or winds to pollutant concentrations, is limited. Thus, studies on this issue are essential to further understand PM$_{2.5}$ pollution and support decision-making related to atmospheric contamination in HCM City, a metropolis of Vietnam.

To identify emission source areas of PM$_{2.5}$, conditional bivariate probability function (CBPF) and hybrid receptor models can be used. The CBPF approach combines pollutant concentrations at receptor site, wind direction, and wind speed to determine emission source areas of pollutants [17]. In addition, the CBPF has been widely used to determine local source areas of air pollutants [18–21] because pollutant dispersion on a local scale (e.g., over a small area) is mainly affected by wind. Added to this, a combination of the CBPF prediction surfaces and their lower/upper 95th confidence intervals should be employed to increase reliability of the emission source areas [22]; however, this approach has not been commonly used in previous studies [18–20]. The hybrid receptor models combine pollutant concentrations and geocoordinates of backward air trajectories arriving at the receptor site; therefore, this model type can be used to identify emission source areas of air pollutants at a non-local scale (e.g., over several hundred to thousands of kilometers from the receptor site) [16,23,24]. Of these models, potential source contribution function (PSCF) and concentration-weighted trajectory (CWT) models have been extensively applied because of their relatively straightforward performance [25]. Particularly, in the PSCF/CWT analysis, the study area is divided into numerous grid cells. The value of each is determined based on the endpoints of air trajectories falling inside each cell together with the pollutant concentrations associated with the air trajectories [26]. Generally, grid cells with high PSCF/CWT values are suggestive of emission source areas of air pollutants [27].

Recently, three-dimensional (3D) hybrid receptor models, considering longitudes, latitudes, and heights of trajectory segments, have been introduced and widely applied to improve the accuracy of model outputs [18,23,28,29]. One of the approaches is to consider trajectory segments transporting within the air mixing layer [18,30], since air pollutants are well-mixed and diffused in this layer once they are released [31]. Added to this, air trajectory segments higher than the mixing heights are likely to capture air pollutants originated from other source areas [18]. Therefore, the 3D hybrid receptor models (e.g., 3D-PSCF and 3D-CWT), considering vertical transport of trajectory segments, have been reported to

identify emission source areas of air pollutants more effectively. Additionally, uncertainties of the 3D hybrid receptor models should be evaluated to limit the misinterpretation of source areas, which can be stemmed from a small number of trajectory segments [32] and/or trailing effects [16]. In this regard, a weighting function can be used to lower the uncertainty of 3D hybrid receptor models [32] and it has been shown to noticeably affect the output of 3D-PSCF/3D-CWT [18]. However, previous studies mostly used a single set of the weighting functions, which can lead to the omission in identifying emission source areas. Consequently, various sets of the weighting functions should be used to avoid this limitation and provide uncertainty of the 3D hybrid receptor models.

This study aims to identify emission source areas of $PM_{2.5}$ in HCM City at local and non-local scales (i.e., inside and outside the city, respectively), utilizing the CBPF, 3D-PSCF, and 3D-CWT models. In addition, variations in the $PM_{2.5}$ mass concentrations and their relationships with several meteorological parameters (e.g., air temperature, air pressure, and wind speed) are evaluated. Notably, uncertainties of the CBPF and 3D-PSCF/3D-CWT were evaluated based on the upper/lower 95th confidence intervals and the 95% confidence levels, respectively. The findings of this study add to the understanding of identifying emission source areas of $PM_{2.5}$ and to the decision-making related to air pollution reduction in HCM City, a metropolis of Vietnam.

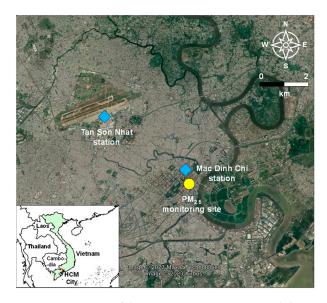## 2. Materials and Methods

2.1. Study Area

Ho Chi Minh (HCM) city has two distinct seasons: the dry season lasting from December to April of the following year and the rainy season covering a period from May to November [4]. The average ambient air temperature and annual rainfall amount of HCM City are approximately 28.4 °C and 2100 mm, respectively [2]. The ambient air temperature of the dry season (28.1–29.3 °C) tends to be higher than that of the rainy season (26.9–27.5 °C) [4]. In addition, the rainfall amount is relatively low in the dry season; however, it rises dramatically in the rainy season and accounts for approximately 80–90% of the total annual rainfall amount, owing to the frequency of rain events in the rainy season [2].

In terms of air pollution, transportation activities have been noted as one of the primary emission sources of air pollutants (e.g., $PM_{2.5}$, NO_x, SO_2, CO, and volatile organic compounds (VOCs)) in HCM City [12,14] due to many vehicles (e.g., approximately 8 million) operating in the city [33]. Furthermore, industrial activities, especially textile and food industrial production, have also been one of the main emission sources of air pollutants in HCM City [12,14,34] because fossil fuels, such as diesel oil and coal, are used in the manufacture of these industrial types [12].

2.2. Data Collection

2.2.1. Mass Concentrations of $PM_{2.5}$

The hourly mass concentrations of $PM_{2.5}$ from 1 January 2019 to 31 December 2020 in this study were obtained from the air pollutant data which are available via the US Environmental Protection Agency (EPA) and the AirNow platform (https://www.airnow.gov/international/, accessed on 15 March 2021), accessed on 15 March 2021. The monitoring site (latitude: 10°47′0.1″ N and longitude: 106°42′2.2″ E) is located at the US Consulate General Ho Chi Minh City in a downtown area of District 1, HCM City (Figure 1). The mass concentrations of $PM_{2.5}$ were determined based on the beta-ray attenuation method [35,36], meaning that the relative shift in the intensity of beta ray passing through un-sampled and sampled filter tapes was used to calculate the mass of $PM_{2.5}$ depositing on the filters [37]. The dataset of $PM_{2.5}$ mass concentrations was firstly checked for invalid values (i.e., QC invalid labeled, missing, negative, and impossibly high values). The invalid data, accounting for 2.99% of the whole dataset, was regarded as null data and filled in using linear interpolation [38]. Consequently, the final dataset had a total number of 17,520 values of the $PM_{2.5}$ mass concentrations.

Figure 1. Location of the PM$_{2.5}$ monitoring site and the meteorological stations in Ho Chi Minh City of Vietnam.

2.2.2. Meteorological Data

Apart from the PM$_{2.5}$ mass concentrations, meteorological data in HCM City (i.e., ambient air temperature, wind speed, wind direction, dewpoint temperature, and air pressure) were also gathered to understand relationships between the meteorological parameters and the PM$_{2.5}$ mass concentrations in HCM City. The hourly data of these meteorological parameters were downloaded from the National Centers for Environmental Information (NCEI) (https://www.ncei.noaa.gov/maps/hourly/, accessed on 15 March 2021) and the selected station is Tan Son Nhat (ID: 4890009999, latitude: 10°49′2″ N, longitude: 106°40′1″ E) (Figure 1). In addition, hourly data of relative humidity in the study period (1 January 2019–31 December 2020) were calculated based on the downloaded data of the ambient air temperature and dewpoint temperature data following Lawrence [39]. Data on the rainfall amount in HCM City during the study period were also obtained from the Mac Dinh Chi station (latitude: 10°47′2″ N, longitude: 106°42′1″ E) (Figure 1), operated by the Hydrometeorological Observatory, Southern region of Vietnam.

2.2.3. Satellite-Derived Data

The satellite-derived data, including aerosol optical depth (AOD) and incoming short-wave flux in the study period (i.e., 1 January 2019 to 31 December 2020), were also collected to support the result interpretation. In particular, this study used the daily AOD at 550 nm with 1 degree spatial resolution from the Moderate Resolution Imaging Spectroradiometer (MODIS) onboard the Terra satellite [40]. The bounding domain for downloading the AOD values was 85°–125° E and 5°–30° N. Additionally, to know the solar radiation intensity in HCM City, hourly data on incoming shortwave flux for 0.5° × 0.625° grid cells over a domain encompassing 10.5°–11° E and 106.5°–107° N were obtained from the Modern-Era Retrospective Analysis for Research and Applications version 2 (MERRA-2) [41]. Moreover, precipitation data over the study area were obtained from the Integrated Multi-satellite Retrievals for Global Precipitation Measurement (GPM IMERG) final product [42] to support the interpretation of PM$_{2.5}$ transport from non-local source areas to HCM City.

2.3. Conditional Bivariate Probability Function (CBPF)

To identify emission source types (e.g., stack and shallow level sources) and emission source areas of PM$_{2.5}$ at a local scale (i.e., inside HCM City), the CBPF tool can be used [17]. This is because diffusion of PM$_{2.5}$ at the local scale (e.g., over a small area) is mostly affected

by wind speed that is associated with the CBPF. The CBPF for the dry and rainy seasons of HCM City were calculated using this equation [17]:

$$\text{CBPF}_{\Delta\theta,\Delta u} = \frac{m_{\Delta\theta,\Delta u}|C \geq x}{n_{\Delta\theta,\Delta u}} \tag{1}$$

where $\Delta\theta$ and Δu indicate wind sector and wind speed, respectively. C is the $PM_{2.5}$ mass concentration higher than threshold x (i.e., 75th percentiles of the $PM_{2.5}$ mass concentrations) connected with wind sector $\Delta\theta$ and wind speed Δu. $m_{\Delta\theta,\Delta u}$ is the number of times the $PM_{2.5}$ mass concentrations in wind sector $\Delta\theta$ and for wind speed Δu greater than the threshold x. $n_{\Delta\theta,\Delta u}$ represents the total number of samples for the corresponding wind sectors and wind speed intervals. Considering the CBPF uncertainty, this study simultaneously used the prediction and uncertainty CBPF plots, showing the predicted emission source areas and the lower or upper 95% confidence intervals, respectively [22]. The CBPF uncertainty plots were computed using the Generalized Additive Model (GAM) [22,43]. The openair package [22] installed in the RStudio Desktop [44], an open-source software, was used to generate the CBPF prediction and uncertainty plots. Generally, the potential source areas contributing to the higher mass concentrations of $PM_{2.5}$ are marked by the high CBPF probabilities. Additionally, areas with similar probabilities between the prediction and uncertainty plots indicate emission source areas having high reliability. On the other hand, the suggested source areas are relatively uncertain due to a lack of data on the corresponding wind speed and wind sector [43].

2.4. Backward Air Trajectory and Trajectory Cluster Analysis

2.4.1. Backward Air Trajectory

The emission source areas of $PM_{2.5}$ on the non-local scale (i.e., outside HCM City) can be identified using the 3D-PSCF and/or 3D-CWT models adopting the backward air trajectory [45]. This study used the Hybrid Single-Particle Lagrangian Integrated Trajectory (HYSPLIT) model version 5.1.0 [46] coupled with Global Data Assimilation System (GDAS1) meteorological data (https://www.ready.noaa.gov/gdas1.php, accessed on 15 March 2021) to simulate the backward air trajectories arriving at the $PM_{2.5}$ monitoring site in HCM City from 1 January 2019 to 31 December 2020. The total run time for backward air trajectory simulation was 96 h (4 days), and the starting heights of the trajectories were set at 50% and 100% of the mixing layer height at the receptor site to acquire high resolution of the hybrid receptor model. A total of 35,040 air trajectories (365 monitoring days × 2 years × 2 starting heights × 24 hrs/day) were used in this study. The uncertainty of air trajectory simulation was also considered by removing trajectory segments exceeded 50% of the mixing layer height [18].

2.4.2. Trajectory Cluster Analysis

To determine the main directions of backward air trajectories, trajectory cluster analysis, performed using TrajStat 1.5.3 [27], was used to group the air trajectories according to their directions and lengths. The Euclidean distance was selected for the clustering and was calculated based on this equation.

$$d_{12} = \sqrt{\sum_{i=1}^{n}[X_1(i) - X_2(i)]^2 + [Y_1(i) - Y_2(i)]^2} \tag{2}$$

where d_{12} indicates the Euclidean distance between two backward trajectories. X_1, X_2 and Y_1, Y_2 represent the latitudes and longitudes of these trajectories, respectively. The fluctuation in the total spatial variance (TSV) was computed to identify the number of clusters, and a significant change in the TSV implies an adequate cluster number [47].

2.5. Three-Dimensional Hybrid Receptor Models

To determine emission source areas of $PM_{2.5}$ in HCM City at the non-local scale (i.e., outside HCM City), this study used the 3D-PSCF and 3D-CWT models, considering

the heights, latitudes, and longitudes of trajectory segments. The 3D-PSCF model was computed following Equation (3) [16].

$$3D - PSCF = \frac{m_{ij}}{n_{ij}} \tag{3}$$

where 3D-PSCF represents the three-dimensional potential source contribution function. m_{ij} is the number of endpoints falling within cell (i,j) when the PM$_{2.5}$ mass concentrations are higher than the threshold values (i.e., 75th percentiles). n_{ij} denotes the number of times the trajectories were processed as described in Section 2.4.

The 3D-CWT model was also computed to confirm the PM$_{2.5}$ emission source areas suggested by the 3D-PSCF and to clarify source areas with high, moderate, and low emissions [16]. The 3D-CWT model was calculated using Equation (4) [16].

$$3D - CWT = \frac{1}{\sum_{l=1}^{M} \tau_{ijl}} \times \sum_{l=1}^{M} \left(C_j \times \tau_{ijl} \right) \tag{4}$$

where M denotes the total number of backward air trajectories, τ_{ijl} is the endpoint number of trajectory l falling in cell (i,j) and processed as described in Section 2.4. C_j is the PM$_{2.5}$ mass concentrations at the receptor site. The 3D-PSCF and 3D-CWT models were performed independently for the dry and wet seasons. In addition, the model outputs were multiplied by weighting functions (W) to reduce uncertainty of the 3D-PSCF and 3D-CWT values stemming from the low values of n_{ij} and τ_{ijl}. The bootstrapping technique was applied to generate the W values by assuming the W to follow data distribution referred in previous studies [18,24,27,29,48]. The W were then simulated repeatedly 500 times before being multiplied by the 3D-PSCF and 3D-CWT values. Following this approach, the 3D-PSCF and 3D-CWT values were also generated 500 times, and their upper confidence levels were reported. The W values and their distribution are shown in Equation (5).

$$W = \begin{cases} 1.00 \text{ (constant distribution)}, & 2s \leq N \\ 0.50\text{--}0.70 \text{ (min} - \text{max distribution)}, & s \leq N < 2s \\ 0.25\text{--}0.42 \text{ (min} - \text{max distribution)}, & 0.5s \leq N < s \\ 0.05\text{--}0.17 \text{ (min} - \text{max distribution)}, & N \leq 0.5s \end{cases} \tag{5}$$

where s is the average number of trajectory endpoints per cell, which are 11 and 30 for the dry and rainy seasons, respectively. N is the total number of trajectory endpoints in each grid cell. The 3D-PSCF and 3D-CWT models were computed for $0.25° \times 0.25°$ grid cells over a domain surrounding 85°–125° E and 5°–25° N using the TrajStat tool [27]. Generally, areas showing the high 3D-PSCF or 3D-CWT values can be considered as possible source areas of PM$_{2.5}$ [16].
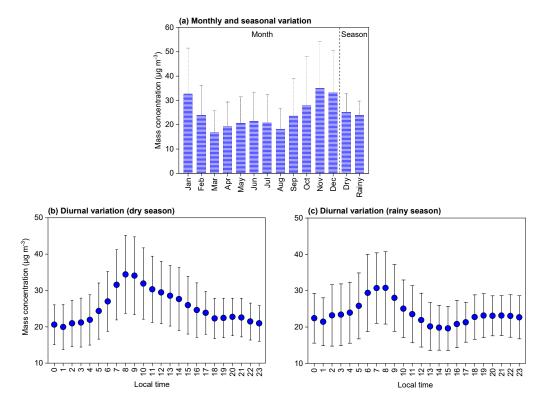
2.6. Data Visualization and Statistical Analysis

The 3D-PSCF and 3D-CWT values were illustrated using ArcMap software version 10.8 (ESRI, USA). In addition, the OriginPro software version 2020 (Origin Lab, USA) was used to plot the PM$_{2.5}$ mass concentrations and values of the meteorological parameters, as well as to conduct the statistical analysis, including the statistical hypothesis test, correlation analysis, and partial least squares regression (PLS). The PLS was used to evaluate the relations between PM$_{2.5}$ mass concentrations and meteorological parameters since this approach can effectively deal with multicollinearity problem [49], which is the linear relationships among independent variables (i.e., the meteorological parameters) in the regression analysis causing less reliable results of the regression model [50].

3. Results and Discussion

3.1. Mass Concentrations of $PM_{2.5}$

In general, the mean of $PM_{2.5}$ mass concentrations in the dry and rainy seasons of HCM City were 25.2 and 23.9 $\mu g\ m^{-3}$, respectively. The relatively lower mass concentrations of $PM_{2.5}$ in the rainy season is contributed by the higher rainfall amount in this season (Figure S1 in the Supplementary Information), removing $PM_{2.5}$ from the atmosphere via wet deposition [51]. In addition, November exhibited the highest mean $PM_{2.5}$ mass concentration (35.1 $\mu g\ m^{-3}$), followed by December (33.4 $\mu g\ m^{-3}$) and January (32.7 $\mu g\ m^{-3}$) (Figure 2a). The lower ambient air temperature of these months (27.6±0.4 °C), compared with the others (28.8 ± 1.0 °C) (Figure S2), can lead to the lower air mixing height in these months (i.e., November, December, and January) [51], enhancing the $PM_{2.5}$ accumulation and resulting in the greater $PM_{2.5}$ mass concentrations in November, December, and January. Moreover, the highest $PM_{2.5}$ mass concentration in November would also be contributed by the temperature inversion, which discourages dispersion of air pollutants and contributes to their higher concentrations [52], since the temperature inversion can more frequently occur in November [53]. The lowest mean concentrations of $PM_{2.5}$ were found in March (16.8 $\mu g\ m^{-3}$), followed by August (18.2 $\mu g\ m^{-3}$) (Figure 2a). These observations are due to the highest wind speeds in March and August (Figure S3) increasing the $PM_{2.5}$ dispersion and leading to a decrease in $PM_{2.5}$ mass concentrations.

Figure 2. Mean of $PM_{2.5}$ mass concentrations in HCM City shown in monthly and seasonal variation, diurnal variation in the dry season, and diurnal variation in the rainy season. The whiskers represent standard deviations of the mean.

In terms of diurnal variation, $PM_{2.5}$ mass concentrations in the dry and rainy seasons of HCM City had a unimodal distribution, with a significant peak in the morning rush hours (i.e., 7:00–9:00 LT) (Figure 2b,c). After this peak, the $PM_{2.5}$ mass concentrations were gradually decreased until late afternoon (e.g., 16:00 LT) and slightly increased around evening rush hours (e.g., 17:00–19:00 LT). Then $PM_{2.5}$ reached the lowest mean concentrations at midnight (e.g., 23:00 to 1:00 LT) and increased gradually to peak around the morning rush hours (e.g., 7:00–9:00 LT) (Figure 2b,c). The highest $PM_{2.5}$ mass concentra-

tions in the morning rush hours of both the dry and rainy seasons are primarily due to the dense automobiles (e.g., bus, car, and motorbike) during this period [54,55]. Transportation activities have also been mentioned as an important emission source of $PM_{2.5}$ in HCM City [12,56]. Furthermore, the lower $PM_{2.5}$ mass concentration after the morning rush hours until late afternoon (e.g., 16:00 LT) can be due to a decline in vehicle exhaust after rush hours and an expansion of planetary boundary layer, enhancing the diffusion of air pollutants during daytime [51].

Notably, no obvious peaks in the $PM_{2.5}$ mass concentrations were observed in the evening rush hours (e.g., 17:00–18:00 LT) (Figure 2b,c) when the significant vehicle density also occurs. This finding is consistent with previous studies on $PM_{2.5}$ pollution in HCM City [5] and suggests that the highest $PM_{2.5}$ mass concentrations in the morning rush hours might be affected by not only vehicle emissions but also other factors, such as secondary organic aerosol (SOA). The SOA can be formed from the nucleation or condensation of pre-existing particles [57,58] and oxidation of VOCs [59]. The VOCs can be originated from transportation activities [60] and can react with free radicals, such as OH, O_3, and NO_3, to form low-volatility products, subsequently condensing onto particles to form SOA [61,62]. Moreover, the higher solar radiation in the morning (Figure S4) would promote the formation of radicals (i.e., OH, O_3, and NO_3) through photochemical reactions [63], and thus, increase the SVOCs oxidation to form more SOA.

The $PM_{2.5}$ mass concentrations observed in this study were compared with those in previous studies on $PM_{2.5}$ pollution in Vietnam and other countries in Southeast Asia. Generally, the mass concentrations of $PM_{2.5}$ in HCM City were approximately 3 times lower than those in Ha Noi City, the capital of Vietnam [64,65], and were comparable with those in some other cities of Southeast Asia, such as Bangkok in Thailand [66,67] Bandung in Indonesia [68] and Kuala Lumpur in Malaysia [69]. More information about this comparison is shown in Table S1. In addition, the relationships between several meteorological parameters and the $PM_{2.5}$ mass concentrations were evaluated using the PLS approach and correlation analysis. Briefly, wind speed showed the significantly negative relations with the $PM_{2.5}$ mass concentrations in the dry and rainy seasons (Figures S5 and S6). The relative humidity and ambient air temperature also had the remarkably negative relations to the $PM_{2.5}$ mass concentrations, especially in the rainy season (Figures S5 and S6). More discussion on this issue is presented in Text S1.

3.2. Local Emission Source Areas of $PM_{2.5}$

The CBPF plots for identifying emission source areas of $PM_{2.5}$ at the local scale (i.e., inside HCM City) are shown in Figure 3. Three same-scale plots were simultaneously considered, including the prediction plot illustrating the predicted areas, the lower and upper uncertainty plots presenting the lower and upper limits of the 95% confidence intervals, respectively. As shown in Figure 3, the CBPF prediction plots of the dry and rainy seasons had the highest probabilities associated with relatively low wind speed (i.e., <3 m/s), suggesting shallow or common ground sources of $PM_{2.5}$ (e.g., vehicle and household emissions) [17] as low wind speed tends to disperse $PM_{2.5}$ over a small area [20]. This result is supported by previous studies also noting that particulate matters (i.e., PM_{10} and $PM_{2.5}$) in HCM City have been primarily emitted from on-road emission sources, such as exhaustion from motorcycles (e.g., cars, buses, and trucks) [12,70].
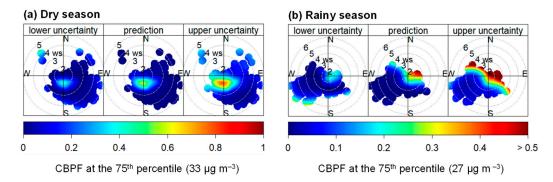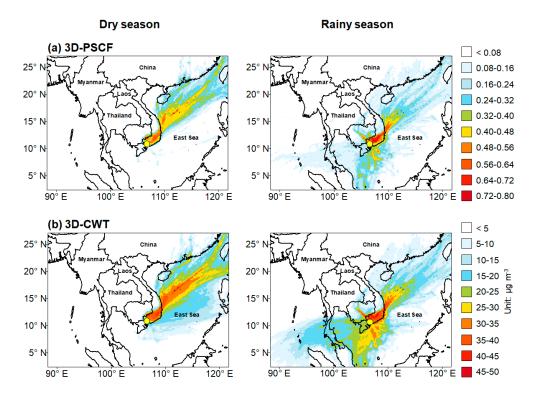
(a) Dry season

(b) Rainy season

Figure 3. CBPF plots of PM$_{2.5}$ in the dry and rainy seasons of HCM City during the study period.
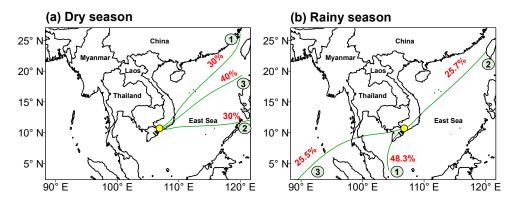
Taking in account the CBPF uncertainty, the lower and upper uncertainty plots of the dry season showed similar areas to the prediction plot (Figure 3a), indicating that the PM$_{2.5}$ emission sources of the dry season (i.e., shallow or common ground sources) were real and not an artifact due to a lack of PM$_{2.5}$ mass concentrations observed in the corresponding wind speeds and wind sectors [17,22]. For the rainy season, the upper uncertainty plot of this season highlighted the PM$_{2.5}$ sources at the southeast and northwest associated with high wind speed (i.e., >3 m/s) (Figure 3b). These sources might be stack emissions [17] from the industrial zones located in the southeast and northwest of HCM City, such as the Linh Trung, Binh Chieu, and Tan Tao industrial zones [12]. Industrial activities in these zones (e.g., textile and food manufacturing) [12] emit a large amount of PM$_{2.5}$ since their production uses fuel (e.g., diesel oil, coal, and wood), one of the major sources of PM$_{2.5}$ [60]. In addition, PM$_{2.5}$ originated from these industrial zones is transported to the monitoring site by the seasonal wind (Figure S7). However, the high CBPF probabilities of the southeast and northwest areas were only shown in the upper uncertainty CBPF plot (Figure 3b); therefore, PM$_{2.5}$ emission sources in these areas might be uncertain due to a lack of observation data in the corresponding wind sectors and wind speeds [43]. Thus, further studies are essential to confirm the PM$_{2.5}$ emission sources in southeast and northwest of HCM City in the rainy season.

3.3. Non-Local Emission Source Areas of PM$_{2.5}$

The emission source areas of PM$_{2.5}$ at a non-local scale (i.e., outside HCM City) were identified using the 3D-PSCF and 3D-CWT models considering longitudes, latitudes, and heights of trajectory segments (Figure 4). In general, areas showing the higher 3D-PSCF and the 3D-CWT values are possibly regarded as emission source areas of PM$_{2.5}$ at the receptor site [71]. In other words, PM$_{2.5}$ originated from these areas can be transported to the receptor site by air masses. Regarding the dry season, an increase in PM$_{2.5}$ mass concentrations at the receptor site in HCM City are contributed by PM$_{2.5}$ emitted from the East Sea (i.e., from shipping emissions) and the southeastern Vietnam (Figure 4), covering some provinces with several industrial zones, such as Dong Nai and Binh Duong provinces [2] (Figure S8). The productions emitting a large of amount of PM$_{2.5}$ in such industrial zones of these provinces are textile and food industries, metal, plastic, and paper productions, wood processing, and construction [2]. In addition, results from the trajectory cluster analysis revealed that in the dry season air trajectories arriving at the receptor site in HCM City mostly came from the southeastern Vietnam (i.e., 70% of the total air masses) (Figure 5). Added to this, the mean of PM$_{2.5}$ mass concentrations corresponding to each trajectory cluster showed the higher values when air parcels came from the southeastern Vietnam (Table S2). These observations emphasized the contribution of PM$_{2.5}$ emission sources in the southeastern Vietnam (e.g., industrial zones in some provinces, such as Binh Duong and Dong Nai) to the elevation of PM$_{2.5}$ mass concentrations in HCM City.

Figure 4. Bootstrapped 3D-PSCF and 3D-CWT results for PM$_{2.5}$ at the 95% upper confidence levels in the dry and rainy seasons. The yellow circles represent the receptor site in HCM City.

Figure 5. Trajectory cluster analysis plots of PM$_{2.5}$ in the dry and rainy seasons of HCM City. The numbers in each circle indicate cluster number. The percentages represent the contribution of each trajectory cluster.

For the rainy season, the 3D-PSCF and 3D-CWT results also suggested the East Sea and southeastern Vietnam as possible source areas of PM$_{2.5}$ at the receptor site in HCM City (Figure 4). However, these sources might have less effect on the PM$_{2.5}$ mass concentrations in HCM City in the rainy season because air parcels arriving from the southeast contributed to approximately 26% of the total air trajectories reaching the monitoring site in the rainy season (Figure 5b). In addition, the 3D-PSCF and 3D-CWT also highlighted the Mekong Delta, located southwest of HCM City (Figure S8), as the potential source area of PM$_{2.5}$ in HCM City in the rainy season (Figure 4). The air masses passing by the Mekong Delta accounted for over 70% of the total air trajectories reaching the receptor site in this season (Figure 5b). Additionally, AOD values over the Mekong Delta were high in the rainy season (Figure S9), which could be because of biomass-burning activities (e.g., burning straw and crop residuals) after harvesting the summer–autumn rice crops (i.e., around June–September) [5]. These findings indicate that PM$_{2.5}$ originated from the Mekong Delta

can transported to HCM City by air masses. However, it should be noted that during the rainy season, transport of $PM_{2.5}$ (i.e., middle- or long-range transport) from outside (i.e., the Mekong Delta and southeastern Vietnam) to HCM City is affected by wet deposition of $PM_{2.5}$ caused by the high rainfall amount over southern Vietnam, including HCM City and its surrounding regions (Figure S10). Thus, the contributions of non-local emission sources to the $PM_{2.5}$ pollution in HCM City during the rainy season can be less important compared with those of the local emission sources (e.g., vehicle emissions).

4. Conclusions

In this study, the local and non-local source areas of $PM_{2.5}$ in HCM City, Vietnam, were identified using the CBPF and 3D-PSCF/3D-CWT models. Uncertainties of these models were evaluated using the upper/lower 95th confidence intervals of the CBPF prediction surfaces and the 95% upper confidence levels, computed from the dataset of 3D-PSCF/3D-CWT generated using the bootstrap technique. Additionally, the mass concentrations of $PM_{2.5}$ and their relationships with meteorological parameters (e.g., air temperature, air pressure, and wind speed) were evaluated. The results showed that the $PM_{2.5}$ mass concentrations in the dry season were higher than those in the rainy season because of the deposition of $PM_{2.5}$ caused by the high rainfall amount during rainy season. For the diurnal variation, the $PM_{2.5}$ mass concentrations in HCM City followed a unimodal distribution, with a significant peak in the morning rush hours (i.e., 7:00–9:00 LT) due to a contribution of SOA, which can be formed in the morning of HCM City.

Regarding the local source areas, the CBPF revealed that $PM_{2.5}$ in HCM City was mainly emitted from shallow or common ground sources (e.g., vehicle and household emissions) throughout the year. Additionally, $PM_{2.5}$ emitted in the northwest and southeast of HCM City might be transported to the receptor site in the rainy season. However, these emission source areas have uncertainty due to a lack of data, thus, further studies are essential to confirm our findings.

In terms of the non-local source areas, $PM_{2.5}$ originated in the East Sea (i.e., from shipping emissions) and southeastern Vietnam (e.g., from several industrial zones in the region) can transported to HCM City, especially in the dry season. Additionally, in the rainy season, the Mekong Delta, located southwest of HCM City, might be the emission source area of $PM_{2.5}$ in this city. However, the contributions of non-local sources to the $PM_{2.5}$ pollution in HCM City might be less important in the rainy season because $PM_{2.5}$ can be removed from the air during its transport as a result of wet deposition under the effect of the large rainfall amount and great rain event frequency during the rainy season. Results from this study can add more information on the identification of emission source areas of air pollutants as well as support decision-making related to the reduction in $PM_{2.5}$ pollution in Vietnam.

References

1. ADB. *Vietnam: Validation of the Country Partnership Strategy Final Review, 2016–2020*; Asian Development Bank (ADB): Mandaluyong, Philippines, 2021.
2. MONRE. *Report of the National Environmental Status*; Ministry of Natural Resources and Environment of Vietnam (MONRE): Ha Noi, Vietnam, 2021.
3. WBG. *Climate Risk Country Profile: Vietnam*; The World Bank Group and Asian Developement Bank: Manila, Philippines, 2021.
4. DONRE. *Report of the Environmental Status of Ho Chi Minh City*; Department of Natural Resources and Environment (DONRE): Ho Chi Minh, Vietnam, 2021.
5. Hien, T.T.; Chi, N.D.T.; Nguyen, N.T.; Vinh, L.X.; Takenaka, N.; Huy, D.H. Current status of fine particulate matter ($PM_{2.5}$) in Vietnam's most populous city, Ho Chi Minh City. *Aerosol Air Qual. Res.* **2019**, *19*, 2239–2251. [CrossRef]
6. Le, T.G.; Ngo, L.; Mehta, S.; Do, V.D.; Thach, T.Q.; Vu, X.D.; Nguyen, D.T.; Cohen, A. Effects of short-term exposure to air pollution on hospital admissions of young children for acute lower respiratory infections in Ho Chi Minh City, Vietnam. *Res. Rep. (Health Eff. Inst.)* **2012**, *169*, 5–72.
7. Toriyama, K.; Fukae, K.; Suda, Y.; Kiyose, T.; Oda, T.; Fujii, Y.; Doan Thien Chi, N.; Huu Huy, D.; Thi Hien, T.; Takenaka, N. NO_2 and HONO concentrations measured with filter pack sampling and high $HONO/NO_2$ ratio in Ho Chi Minh city, Vietnam. *Atmos. Res.* **2019**, *214*, 116865. [CrossRef]
8. WHO. *WHO Global Air Quality Guidelines: Particulate Matter (PM2.5 and PM10), Ozone, Nitrogen Dioxide, Sulfur Dioxide and Carbon Monoxide*; WHO (World Health Organization): Geneva, Switzerland, 2021.
9. MONRE. *National Technical Regulation on Ambient Air Quality (QCVN 05:2013/BTNMT)*; MONRE (Ministry of Natuaral Resources and Environmemt): Ha Noi, Vietnam, 2013.
10. Adgate, J.L.; Mongin, S.J.; Pratt, G.C.; Zhang, J.; Field, M.P.; Ramachandran, G.; Sexton, K. Relationships between personal, indoor, and outdoor exposures to trace elements in $PM_{2.5}$. *Sci. Total Environ.* **2007**, *386*, 21–32. [CrossRef]
11. Xing, Y.-F.; Xu, Y.-H.; Shi, M.-H.; Lian, Y.-X. The impact of $PM_{2.5}$ on the human respiratory system. *J. Thorac. Dis.* **2016**, *8*, E69–E74. [CrossRef]
12. Ho, Q.B.; Vu, H.N.K.; Nguyen, T.T.; Nguyen, T.T.H.; Nguyen, T.T.T. A combination of bottom-up and top-down approaches for calculating of air emission for developing countries: A case of Ho Chi Minh City, Vietnam. *Air Qual. Atmos. Health* **2019**, *12*, 1059–1072. [CrossRef]
13. Nguyen, T.T.Q.; Takeuchi, W.; Misra, P.; Hayashida, S. Technical note: Emission mapping of key sectors in Ho Chi Minh City, Vietnam, using satellite-derived urban land use data. *Atmos. Chem. Phys.* **2021**, *21*, 2795–2818. [CrossRef]
14. Ho, B.Q.; Vu, K.H.N.; Nguyen, T.T.; Nguyen, H.T.T.; Ho, D.M.; Nguyen, H.N.; Nguyen, T.T.T. Study loading capacties of air pollutant emissions for developing countries: A case of Ho Chi Minh City, Vietnam. *Sci. Rep.* **2020**, *10*, 5827. [CrossRef]
15. Huy, D.H.; Hien, T.T.; Takenaka, N. Influence of urban outflow on water-soluble ions in $PM_{2.5}$ and >$PM_{2.5}$ particles at a suburban Ho Chi Minh City site, Vietnam. *Atmos. Res.* **2022**, *272*, 106144. [CrossRef]
16. Hsu, Y.-K.; Holsen, T.M.; Hopke, P.K. Comparison of hybrid receptor models to locate PCB sources in Chicago. *Atmos. Res.* **2003**, *37*, 545–562. [CrossRef]
17. Uria-Tellaetxe, I.; Carslaw, D.C. Conditional bivariate probability function for source identification. *Environ. Model. Softw.* **2014**, *59*, 1–9. [CrossRef]
18. Nguyen, T.N.T.; Vuong, Q.T.; Lee, S.-J.; Xiao, H.; Choi, S.-D. Identification of source areas of polycyclic aromatic hydrocarbons in Ulsan, South Korea, using hybrid receptor models and the conditional bivariate probability function. *Environ. Sci. Process. Impacts* **2022**, *24*, 140–151. [CrossRef]
19. Ali-Taleshi, M.S.; Moeinaddini, M.; Riyahi Bakhtiari, A.; Feiznia, S.; Squizzato, S.; Bourliva, A. A one-year monitoring of spatiotemporal variations of $PM_{2.5}$-bound PAHs in Tehran, Iran: Source apportionment, local and regional sources origins and source-specific cancer risk assessment. *Environ. Pollut.* **2021**, *274*, 115883. [CrossRef]
20. Mukherjee, A.; Agrawal, M. Assessment of local and distant sources of urban $PM_{2.5}$ in middle Indo-Gangetic plain of India using statistical modeling. *Atmos. Res.* **2018**, *213*, 275–287. [CrossRef]
21. Squizzato, S.; Cazzaro, M.; Innocente, E.; Visin, F.; Hopke, P.K.; Rampazzo, G. Urban air quality in a mid-size city—$PM_{2.5}$ composition, sources and identification of impact areas: From local to long range contributions. *Atmos. Res.* **2017**, *186*, 51–62. [CrossRef]
22. Carslaw, D.C.; Ropkins, K. openair—An R package for air quality data analysis. *Environ. Modell. Softw.* **2012**, *27–28*, 52–61. [CrossRef]

23. Kim, I.S.; Wee, D.; Kim, Y.P.; Lee, J.Y. Development and application of three-dimensional potential source contribution function (3D-PSCF). *Environ. Sci. Pollut. Res.* **2016**, *23*, 16946–16954. [CrossRef]

24. Cai, Q.; Tong, L.; Zhang, J.; Zheng, J.; He, M.; Lin, J.; Chen, X.; Xiao, H. Characteristics of long-range transported $PM_{2.5}$ at a coastal city using the single particle aerosol mass spectrometry. *Environ. Eng. Res.* **2019**, *24*, 690–698. [CrossRef]

25. Wang, Y.Q. An open source software suite for multi-dimensional meteorological data computation and visualisation. *J. Open Res. Softw.* **2019**, *7*, 21. [CrossRef]

26. Fan, A.; Hopke, P.K.; Raunemaa, T.M.; Öblad, M.; Pacyna, J.M. A study on the potential sources of air pollutants observed at Tjörn, Sweden. *Environ. Sci. Pollut. Res.* **1995**, *2*, 107–115. [CrossRef]

27. Wang, Y.Q.; Zhang, X.Y.; Draxler, R.R. TrajStat: GIS-based software that uses various trajectory statistical analysis methods to identify potential sources from long-term air pollution measurement data. *Environ. Modell. Softw.* **2009**, *24*, 938–939. [CrossRef]

28. Kim, I.S.; Lee, J.Y.; Wee, D.; Kim, Y.P. Estimation of the contribution of biomass fuel burning activities in North Korea to the air quality in Seoul, South Korea: Application of the 3D-PSCF method. *Atmos. Res.* **2019**, *230*, 104628. [CrossRef]

29. Dimitriou, K.; Grivas, G.; Liakakou, E.; Gerasopoulos, E.; Mihalopoulos, N. Assessing the contribution of regional sources to urban air pollution by applying 3D-PSCF modeling. *Atmos. Res.* **2021**, *248*, 105187. [CrossRef]

30. Stojić, A.; Stanišić Stojić, S. The innovative concept of three-dimensional hybrid receptor modeling. *Atmos. Res.* **2017**, *164*, 216–223. [CrossRef]

31. Wagner, P.; Schäfer, K. Influence of mixing layer height on air pollutant concentrations in an urban street canyon. *Urban Clim.* **2017**, *22*, 64–79. [CrossRef]

32. Pekney, N.J.; Davidson, C.I.; Zhou, L.; Hopke, P.K. Application of PSCF and CPF to PMF-modeled sources of PM2.5 in Pittsburgh. *Aerosol Sci. Technol.* **2006**, *40*, 952–961. [CrossRef]

33. Vu, H.N.K.; Ha, Q.P.; Nguyen, D.H.; Nguyen, T.T.T.; Nguyen, T.T.; Nguyen, T.T.H.; Tran, N.D.; Ho, B.Q. Poor air quality and its association with mortality in Ho Chi Minh City: Case Study. *Atmosphere* **2020**, *11*, 750. [CrossRef]

34. Ho, B.Q.; Khue Vu, H.N.; Nguyen, T.T.; Nguyen, T.-T.G.; Diep, T.-Q.N.; Vo, P.L.; Pham, T.-K.N. Modeling impacts of industrial park activity on air quality of surrounding area for identifying isolation distance: A case of Tan Tao Industrial Park, Ho Chi Minh City, Viet Nam. *IOP Conf. Ser. Earth Environ. Sci.* **2022**, *964*, 012023. [CrossRef]

35. Mukherjee, A.; Toohey, D.W. A study of aerosol properties based on observations of particulate matter from the U.S. Embassy in Beijing, China. *Earth's Future* **2016**, *4*, 381–395. [CrossRef]

36. Ali, S.M.; Malik, F.; Anjum, M.S.; Siddiqui, G.F.; Anwar, M.N.; Lam, S.S.; Nizami, A.-S.; Khokhar, M.F. Exploring the linkage between $PM_{2.5}$ levels and COVID-19 spread and its implications for socio-economic circles. *Environ. Res.* **2021**, *193*, 110421. [CrossRef]

37. Shukla, K.; Aggarwal, S.G. A technical overview on beta-attenuation method for the monitoring of particulate matter in ambient air. *Aerosol Air Qual. Res.* **2022**, *22*, 220195. [CrossRef]

38. Huang, G. Missing data filling method based on linear interpolation and lightgbm. *J. Phys. Conf. Ser.* **2021**, *1754*, 012187. [CrossRef]

39. Lawrence, M.G. The relationship between relative humidity and the dewpoint temperature in moist air: A simple conversion and applications. *Bull. Am. Meteorol. Soc.* **2005**, *86*, 225–234. [CrossRef]

40. Platnick, S. MODIS Atmosphere L3 Monthly Product. NASA MODIS Adaptive Processing System, Goddard Space Flight Center, USA. 2015. Available online: http://dx.doi.org/10.5067/MODIS/MOD08_M3.006 (accessed on 1 February 2022).

41. Global Modeling and Assimilation Office (GMAO). MERRA-2 tavg1_2d_rad_Nx: 2d,1-Hourly, Time-Averaged, Single-Level, Assimilation, Radiation Diagnostics V5.12.4, Greenbelt, MD, USA, Goddard Earth Sciences Data and Information Services Center (GES DISC). 2015. Available online: https://disc.gsfc.nasa.gov/datasets/M2T1NXRAD_5.12.4/summary (accessed on 1 February 2022).

42. Huffman, G.J.; Stocker, E.F.; Bolvin, D.T.; Nelkin, E.J.; Tan, J. GPM IMERG Final Precipitation L3 1 day 0.1 degree x 0.1 degree V06, Edited by Andrey Savtchenko, Greenbelt, MD, Goddard Earth Sciences Data and Information Services Center (GES DISC). 2019. Available online: https://catalog.data.gov/dataset/gpm-imerg-final-precipitation-l3-1-day-0-1-degree-x-0-1-degree-v06-gpm-3imergdf-at-ges-dis (accessed on 1 February 2022).

43. Jeričević, A.; Gašparac, G.; Mikulec, M.M.; Kumar, P.; Prtenjak, M.T. Identification of diverse air pollution sources in a complex urban area of Croatia. *J. Environ. Manag.* **2019**, *243*, 67–77. [CrossRef]

44. Team, R. RStudio: Integrated Development for R. Available online: http://www.rstudio.com/ (accessed on 1 February 2022).

45. Simmonds, P.G.; Seuring, S.; Nickless, G.; Derwent, R.G. Segregation and interpretation of ozone and carbon monoxide measurements by air mass origin at the TOR station mace head, Ireland from 1987 to 1995. *J. Atmos. Chem.* **1997**, *28*, 45–59. [CrossRef]

46. Stein, A.F.; Draxler, R.R.; Rolph, G.D.; Stunder, B.J.B.; Cohen, M.D.; Ngan, F. NOAA's HYSPLIT atmospheric transport and dispersion modeling system. *Bull. Am. Meteorol. Soc.* **2015**, *96*, 2059–2077. [CrossRef]

47. Edwards, A.W.F.; Cavalli-Sforza, L.L. A method for cluster analysis. *Biometrics* **1965**, *21*, 362–375. [CrossRef]

48. Zong, Z.; Wang, X.; Tian, C.; Chen, Y.; Fu, S.; Qu, L.; Ji, L.; Li, J.; Zhang, G. PMF and PSCF based source apportionment of $PM_{2.5}$ at a regional background site in North China. *Atmos. Res.* **2018**, *203*, 207–215. [CrossRef]

49. Wondola, D.; Aulele, S.; Lembang, F. Partial Least Square (PLS) method of addressing multicollinearity problems in multiple linear regressions (Case studies: Cost of electricity bills and factors affecting it). *J. Phys. Conf. Ser.* **2020**, *1463*, 012006. [CrossRef]

50. Čulić, V. Triggering of cardiac arrhythmias. *J. Am. Coll. Cardiol.* **2014**, *63*, 1226–1227. [CrossRef]

51. Chen, Z.; Chen, D.; Zhao, C.; Kwan, M.-P.; Cai, J.; Zhuang, Y.; Zhao, B.; Wang, X.; Chen, B.; Yang, J.; et al. Influence of meteorological conditions on PM$_{2.5}$ concentrations across China: A review of methodology and mechanism. *Environ. Int.* **2020**, *139*, 105558. [CrossRef]

52. Gramsch, E.; Cáceres, D.; Oyola, P.; Reyes, F.; Vásquez, Y.; Rubio, M.A.; Sánchez, G. Influence of surface and subsidence thermal inversion on PM$_{2.5}$ and black carbon concentration. *Atmos. Res.* **2014**, *98*, 290–298. [CrossRef]

53. Nam, N.T.T.; Trinh, N.N.; Thu, N.T.M.; Bảo, P.T. Characteristics and effect of the temperature inversion on concentrations of fine particulate matter (PM2.5) in Ho Chi Minh city, Vietnam. *J. Hydro-Meteorol.* **2023**, *746*, 87–95. [CrossRef]

54. Pushpawela, B.; Shelton, S.; Liyanage, G.; Jayasekara, S.; Rajapaksha, D.; Jayasundara, A.; Jayasuriya, L.D. Changes of Air Pollutants in Urban Cities during the COVID-19 Lockdown-Sri Lanka. *Aerosol Air Qual. Res.* **2023**, *23*, 220223. [CrossRef]

55. Shelton, S.; Liyanage, G.; Jayasekara, S.; Pushpawela, B.; Rathnayake, U.; Jayasundara, A.; Jayasooriya, L.D. Seasonal Variability of Air Pollutants and Their Relationships to Meteorological Parameters in an Urban Environment. *Adv. Meteorol.* **2022**, *2022*, 5628911. [CrossRef]

56. Huong Giang, N.T.; Kim Oanh, N.T. Roadside levels and traffic emission rates of PM$_{2.5}$ and BTEX in Ho Chi Minh City, Vietnam. *Atmos. Environ.* **2014**, *94*, 806–816. [CrossRef]

57. Liang, L.; Engling, G.; Cheng, Y.; Zhang, X.; Sun, J.; Xu, W.; Liu, C.; Zhang, G.; Xu, H.; Liu, X.; et al. Influence of high relative humidity on secondary organic carbon: Observations at a background site in East China. *J. Meteorol. Res.* **2019**, *33*, 905–913. [CrossRef]

58. Pushpawela, B.; Jayaratne, R.; Morawska, L. The influence of wind speed on new particle formation events in an urban environment. *Atmos. Res.* **2019**, *215*, 37–41. [CrossRef]

59. Shrivastava, M.; Cappa, C.D.; Fan, J.; Goldstein, A.H.; Guenther, A.B.; Jimenez, J.L.; Kuang, C.; Laskin, A.; Martin, S.T.; Ng, N.L.; et al. Recent advances in understanding secondary organic aerosol: Implications for global climate forcing. *Rev. Geophys.* **2017**, *55*, 509–559. [CrossRef]

60. Harrison, R.M.; Allan, J.; Carruthers, D.; Heal, M.R.; Lewis, A.C.; Marner, B.; Murrells, T.; Williams, A. Non-exhaust vehicle emissions of particulate matter and VOC from road traffic: A review. *Atmos. Res.* **2021**, *262*, 118592. [CrossRef]

61. Kroll, J.H.; Seinfeld, J.H. Chemistry of secondary organic aerosol: Formation and evolution of low-volatility organics in the atmosphere. *Atmos. Res.* **2008**, *42*, 3593–3624. [CrossRef]

62. Pushpawela, B.; Jayaratne, R.; Morawska, L. Differentiating between particle formation and growth events in an urban environment. *Atmos. Chem. Phys.* **2018**, *18*, 11171–11183. [CrossRef]

63. Sadanaga, Y.; Matsumoto, J.; Kajii, Y. Photochemical reactions in the urban air: Recent understandings of radical chemistry. *J. Photochem. Photobiol. C Photochem. Rev.* **2003**, *4*, 85–104. [CrossRef]

64. Hai, C.D.; Kim Oanh, N.T. Effects of local, regional meteorology and emission sources on mass and compositions of particulate matter in Hanoi. *Atmos. Res.* **2013**, *78*, 105–112. [CrossRef]

65. Thuy, N.T.T.; Dung, N.T.; Sekiguchi, K.; Thuy, L.B.; Hien, N.T.T.; Yamaguchi, R. Mass concentrations and carbonaceous compositions of PM$_{1.0}$, PM$_{2.5}$, and PM$_{10}$ at urban locations of Hanoi, Vietnam. *Aerosol Air Qual. Res.* **2018**, *18*, 1591–1605. [CrossRef]

66. Oanh, N.T.K.; Kongpran, J.; Hang, N.T.; Parkpian, P.; Hung, N.T.Q.; Lee, S.B.; Bae, G.N. Characterization of gaseous pollutants and PM2.5 at fixed roadsides and along vehicle traveling routes in Bangkok Metropolitan Region. *Atmos. Res.* **2013**, *77*, 674–685.

67. ChooChuay, C.; Pongpiachan, S.; Tipmanee, D.; Suttinun, O.; Deelaman, W.; Wang, Q.; Xing, L.; Li, G.; Han, Y.; Palakun, J.; et al. Impacts of PM$_{2.5}$ sources on variations in particulate chemical compounds in ambient air of Bangkok, Thailand. *Atmos. Pollut. Res.* **2020**, *11*, 1657–1667. [CrossRef]

68. Sinaga, D.; Setyawati, W.; Cheng, F.Y.; Lung, S.-C.C. Investigation on daily exposure to PM2.5 in Bandung city, Indonesia using low-cost sensor. *J. Expo. Sci. Environ. Epidemiol.* **2020**, *30*, 1001–1012. [CrossRef]

69. Khan, M.F.; Sulong, N.A.; Latif, M.T.; Nadzir, M.S.M.; Amil, N.; Hussain, D.F.M.; Lee, V.; Hosaini, P.N.; Shaharom, S.; Yusoff, N.A.Y.M.; et al. Comprehensive assessment of PM$_{2.5}$ physicochemical properties during the Southeast Asia dry season (southwest monsoon). *J. Geophys. Res. Atmos.* **2016**, *121*, 14,589–14,611. [CrossRef]

70. Nguyen, D.L.; Czech, H.; Pieber, S.M.; Schnelle-Kreis, J.; Steinbacher, M.; Orasche, J.; Henne, S.; Popovicheva, O.B.; Abbaszade, G.; Engling, G.; et al. Carbonaceous aerosol composition in air masses influenced by large-scale biomass burning: A case study in northwestern Vietnam. *Atmos. Chem. Phys.* **2021**, *21*, 8293–8312. [CrossRef]

71. Hsu, Y.-K.; Holsen, T.M.; Hopke, P.K. Locating and quantifying PCB sources in Chicago: Receptor modeling and field sampling. *Environ. Sci. Technol.* **2003**, *37*, 681–690. [CrossRef]